Journal of the Korean Physical Society, Vol. 54, No. 2, February 2009, pp. 592∼596

Multi-Segment Position-Sensitive Detector for an X-ray Imaging Crystal Spectrometer

Jong Kyu Cheon
Neutron Science Division, Korea Atomic Energy Research Institute, Daejeon 305-353 and Department of Physics, Kyungpook National University, Daegu 702-701

Myung Kook Moon* and Chang Hee Lee
Neutron Science Division, Korea Atomic Energy Research Institute, Daejeon 305-353

Shraddha S. Desai
Solid State Physics Division, Bhabha Atomic Research Center, 400 085 Mumbai, India

Uk Won Nam
Space Science Division, Korea Astronomy and Space Science Institute, Daejeon 305-348

Sang Gon Lee and Jun Gyo Bak
KSTAR Experiment and Operation Division, National Fusion Research Institute, Daejeon 305-333

Hee Dong Kang
Department of Physics, Kyungpook National University, Daegu 702-701

(Received 3 November 2008)

A two-dimensional segmented position sensitive detector (PSD) as a part of an X-ray imaging crystal spectrometer (XICS) for use in tokamak plasma experiments was developed. It is based on a multi-wire proportional counter (MWPC) using a delay-line readout method. The MWPC, necessary for recording plasma image data, provides the combined advantages of low neutron radiation sensitivity and large sensitive detection area. The fabricated PSD for the XICS is a four-segment MWPC that can be used in intense X-ray photon environments.

PACS numbers: 29.40.Cs, 52.70.-m
Keywords: MWPC, Segment detector, Rate capability, Plasma diagnosis, XICS

I. INTRODUCTION

X-ray imaging crystal spectrometers (XICS) are important plasma diagnostic instruments that provide ion and electron temperature profiles, toroidal rotation velocities, impurity charge-state distributions and ionization equilibrium measurements [1]. In order to measure ion temperatures in tokamak devices, typically, argon gas is injected into the device, where the high temperature of the plasma ionizes it into helium-like argon (Ar XVII, Ar^{16+}). This helium-like argon then radiates characteristic X-rays. A spherically-bent quartz crystal can then be used to obtain the resulting X-ray spectrum. Due to thermal motion, the helium-like argon atoms have a component of velocity along the line-of-sight of the observer. The emitted X-rays are, thus, Doppler shifted, which results in a line broadening effect that can be expressed as

$$\Delta\lambda = \lambda_0 \sqrt{\frac{kT}{mc^2}}. \quad (1)$$

Here, $\Delta\lambda$, λ_0, k, T, m and c are the Doppler broadening, the central X-ray wavelength (from the helium-like argon), the Boltzmann constant, the ion temperature, the mass of the helium-like argon and the speed of light, respectively. The above relation was derived from the Maxwell distribution and Doppler effect [2–4]. As shown in Eq. (1), the wavelength broadening $\Delta\lambda$ is directly proportional to the square root of the ion temperature T.

Essential components of the XICS are a spherically-bent quartz crystal and a 2D position-sensitive detector

*E-mail: moonmk@kaeri.re.kr;
Tel: +82-42-868-8437; Fax: +82-42-868-4629

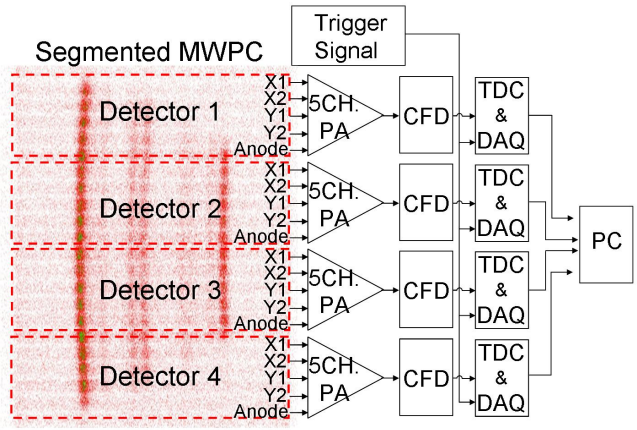

Fig. 1. Block diagram of the four-segment PSD system with improved count-rate capability.

(PSD). The 2D PSD requires a large sensitive area (in excess of 10 cm × 30 cm), a photon counting capability for time-resolved experiments and a position resolution of less than 0.5 mm. In general, contemporary tokamak plasmas generate high fluxes of potentially damaging fast neutrons. The gas-filled multi-wire proportional counter(MWPC) used in this work has the advantage of low susceptibility to radiation damage from these fast neutrons. In addition, the sensitive area of detection of the MWPC can be substantially increased in a cost-effective manner. This improves the performance of the XICS. A proof-of-principal experiment using the XICS (with a conventional un-segmented MWPC) indicated that the X-ray photon count rates were limited to 400 kcps due to the time-to-digital converter (TDC) -based data acquisition system [1,5]. Hence, an improved XICS adopting a segmented MWPC design was fabricated to achieve high X-ray photon count-rates. The fabricated PSD is a four-segment MWPC with a sensitive area of 10 cm × 30 cm.

II. DESIGN AND FABRICATION OF THE DETECTOR

A schematic diagram of the multi-segment detector and its associated time-delay line data acquisition system is presented in Figure 1. The high count-rate X-ray photons originating from the tokamak plasma enter the detector through the XICS. The most important factors in terms of the count-rate capabilities of the MWPC are the space charge effect and the dead time. Space charge effects hamper MWPC's accurate detection of locally intense beams. The local count-rate capability of the MWPC is about 10^4 cps/mm^2 [6]. The space charge effect, which introduces count loss, dominates when the X-ray image exhibits intense spatial localities. One can overcome local count-rate limitations in MWPCs by minimizing the space between the anode (gas multiplication) and the cathode (readout) wires. The PSD micro-strip gas chambers (MSGC) use this method. However, large sensitive-area MSGCs cannot provide long-term stability as they are easily damaged by sparks between the anode and the cathode electrodes. In this work, the gap between the cathode and the anode wires of the MWPC is reduced by 3.2 mm, which can ensure stability.

As mentioned above, the total TDC count-rate from previous investigations saturated at about 400 kcps. However, the maximum output signal count rate from the MWPC preamplifier was about 2 Mcps using a pulse counter. This demonstrates that count loss result not from the MWPC, but from inadequacies in the readout electronics.

Count-rate saturation in the XICS system resulted by a combination of readout electronics inadequacies and spatially large X-ray images. In order to design a PSD capable of resolving larger images, the readout system must be able to handle a larger quantity of data. In order to circumvent count-rate saturation issues, a multi-segment MWPC was employed. It was found to be effective in the environments of concern to us. In Figure 1, the image in the dotted line region is a real image of the helium-like Ar lines recorded from the XICS with a regular un-segmented MWPC [1,5]. As shown in the figure, the detection area is divided into 4 segments, each having its own data acquisition system. Total count-rate capabilities increase because the detection area per segment is reduced, thus lessening the burden on each (now four) channel of the data acquisition. The detector signals of each segment are designated as X1, X2, Y1, Y2 and Anode. Each axis of the segment has two outputs from the cathode frame, which are distinguished by the suffixes 1 and 2. The Anode signal is used as a trigger for the TDC. A constant fraction discriminator (CFD) converts the analog signal from the preamplifiers into a digital signal that is fed into the TDC and data acquisition module (DAQ). All four TDC and DAQ modules are synchronized with a trigger originating from the tokamak. All data from the TDC and the DAQ modules are recorded through an USB interface by using a computer [7].

The measured X-ray energy at the XICS was sufficiently low (3.1 keV) that a thin beryllium foil (thickness ≈0.2 mm) used for the window material of the MWPC proved appropriate. The MWPC was directly installed into the XICS system. As the latter operates under high vacuum, 29 supporting rib-structures were needed (on the detector window) to protect the thin Be window from the large pressure differentials. The multi-segment detector required 20 vacuum-tight coaxial connectors. Hermetically-sealed SMA-type connectors were, thus, selected. They are smaller than BNC connectors, so a larger number of them could be easily accommodated on a given chamber. As previously mentioned, each segment required 5 connectors. Two SHV connectors were mounted for the anode high-voltage bias and

Table 1. Detector parameters.

Delay time	
X axis [ns]	223
Y axis [ns]	158
Number of taps	
X axis	53
Y axis	30
Frame-to-frame distance	
Anode-Upper cathode [mm]	3.2
Lower cathode-Anode [mm]	3.2
Lower cathode-window [mm]	0.8
Anode frame	
Wire thickness [μm]	10
Wire spacing [mm]	2
Upper cathode frame	
Electrode type	Strip line
Lower cathode frame	
Wire thickness [μm]	30
Wire spacing [mm]	1
Detection gas	Kr + C_2H_6(20 %) + CF_4 (1 %) 1 atm

the drift bias. The parameters for each single segment of the detector are shown in Table 1.

All wire frames inside the detector were made with a winding machine, whose provision of equal tension for all wires in the same frame improves the uniformity of gain over the entire sensitive area. All frames inside the MWPC, including the upper cathode frame, the lower cathode and the anode, are separated into four sections (Figure 2(a)) so that each detector segment works independently. The high-voltage electrodes of the anode frame were bridged using DC blocking capacitors and carbon resistors to prevent signal interference. A rear view of the completely assembled 4-segment detector is presented in Figure 2(b).

III. PERFORMANCE TEST

Performance tests of each segment of the four-segment detector, including the operating voltage and the counting efficiencies, were carried out using a Fe^{55} X-ray source located 450 mm from the detector. The segments were uniformly illuminated. The measured counting plateaus for all segments were compared (Figure 3). The optimum operating voltage was found to be 1800 – 2050 V. All four detectors showed similar characteristics. The counting plateau phenomenon for the segmented MWPC is the same as that for the regular un-segmented MWPC. Therefore, individual high-voltage power supplies for each segment of the detector are unnecessary.

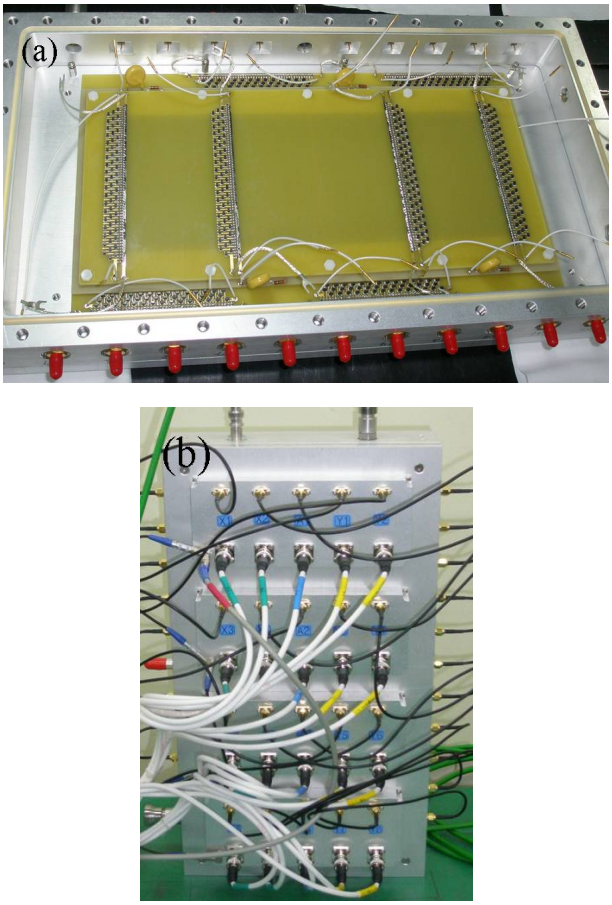

Fig. 2. Fabricated four-segmented PSD. (a) Inside view of the 4-segment detector. (b) Rear view of the 4-segment detector.

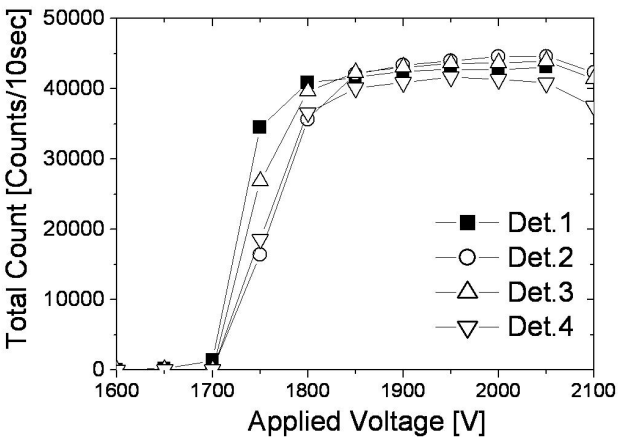

Fig. 3. Counting plateau of the four-segment PSD.

The anode wire spacing for the 2D MWPC limits the position resolution perpendicular to the wire. Note that a relatively narrow-wire MWPC requires relatively high operating voltages for a given avalanche net charge. This increased voltage may increase spurious discharges (and ensuing noise) in the detector.

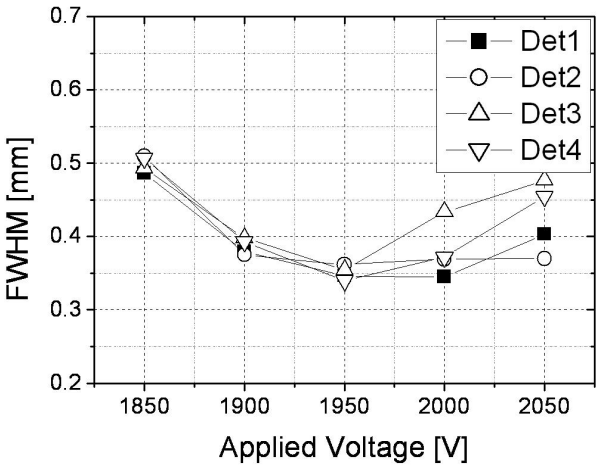

Fig. 4. Position resolution along the X-axis as a function of applied voltage.

The X and the Y axes of the XICS detector provide wavelength and spatial information, respectively. As we are more interested in the ion temperature, which is reflected in wavelength measurements, the position resolution of the X-axis is more important than that of the Y-axis [1]. The position resolution of the fabricated MWPC in the direction of the Y-axis was maintained at about 2 mm to increase the stability of the detector.

The position resolution of the X-axis as a function of the applied voltage using a 30-μm-wide slit was investigated (Figure 4). The best resolution (full width at half maximum: FWHM) was 0.35 mm at a 1950-V applied voltage. Poorer resolution with higher applied voltages results from detector noise. The slightly different FWHM resolutions observed from the 4 segments result from the slit not being exactly perpendicular to the X-axis of each detector.

A simple image test allowed us to investigate the performance of the combined electronics-detector system. A spanner was mounted in front of the detector window and was irradiated with Fe^{55} X-rays (Figure 5(a)). The image of the spanner recorded in all segments confirmed that the entire sensitive area responded well. The protective ribs on the detector show up as thick white (shadow) lines (Figure 5).

As previously mentioned, the X-ray photon counts from the previous experiments using a regular unsegmented MWPC saturated at 400 kcps due to the TDC dead time. The count-rate capabilities of the regular unsegmented and the bi-segmented MWPC [8] were compared (Figure 6). Two Fe^{55} X-ray sources with activities of 10 and 20 mCi were used in this experiment. The count-rate was measured as a function of the source-detector distance, which ranged from 5 to 40 mm. In Figure 6, a counting loss by X-ray absorption in air and a counting gain by a variation of the irradiation area with distance are compensated. The relation between the source-to-detector distance and the X-ray intensity

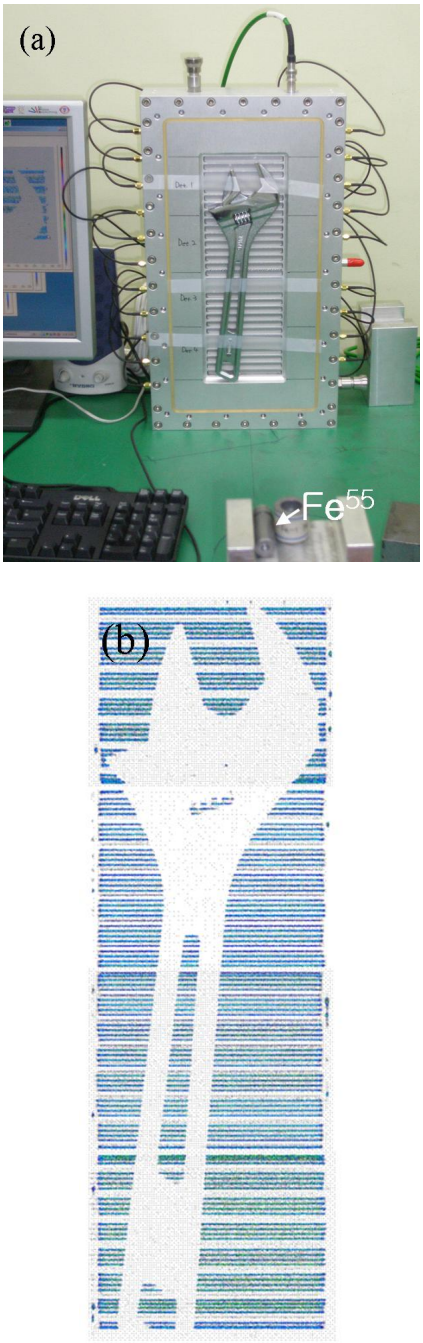

Fig. 5. Full image test of the four-segment PSD system. (a) Recorded spanner image. (b) Spanner image recorded by using the four-segment MWPC.

can be expressed as

$$I \propto 1/x^2, \tag{2}$$

where I and x are the X-ray intensity and the source-detector distance, respectively. From Eq. (2), the measured photon flux decreases as $1/x^2$ [9]. Accordingly, $1/x^2$ is proportional to the true interaction rate of MWPC. For zero system dead-time, the line in Fig-

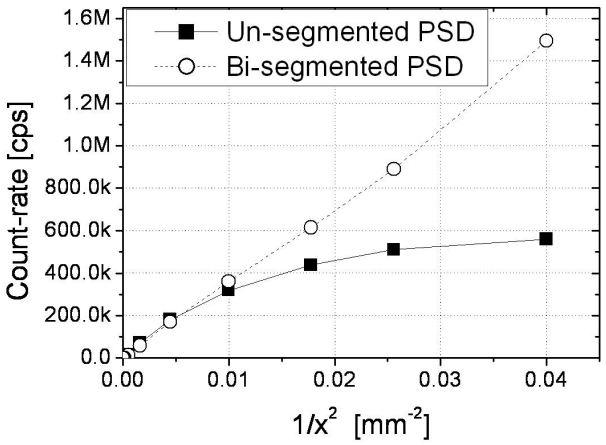

Fig. 6. Count rate capability test with un-segmented and multi-segment detectors.

ure 6 should be linear. Two models of the dead time behavior are the nonparalyzable and paralyzable model, where the latter provides a better model for most TDC systems:

$$m = ne^{-n\tau} \quad \text{Paralyzable model.} \tag{3}$$

Here n, m and τ are the true interaction rate, the recorded count rate and the system dead time, respectively [10]. In this model, m is maximal for $n = 1/\tau$ and it decreases for $n > 1/\tau$.

The un-segmented MWPC count-rate saturated at about 550 kcps, which is higher than the previously measured count-rate limitation (Figure 6). In general, the maximal (MWPC) count-rate depends on the delay time. The TDC gate time is twice the delay time and, thus, is the dead time of the MWPC measurement system used in this work. Dead time loses are severe for high photon count rates. Since the bi-segmented MWPC system has two TDCs (of reduced sensitive area by half of the un-segmented detector), the system dead time is decreased due to the reduction of pulse pile-up. Therefore, a multi-segmented MWPC can increase the count-rate capability by reducing the system dead time and as a result, the measurement curve from the bi-segmented MWPC shows an increased photon count rate of 1.4 Mcps without saturation.

IV. CONCLUSION

A four-segment MWPC for XICS was fabricated and its performance was investigated. The detector proved to be successful, meeting our XICS requirements. Its position resolution was 0.35 mm and its optimum anode voltage was 1950 V. The segmented MWPC had a higher count rate capability than a regular un-segmented PSD through a reduction of the system dead time. In the future, we plan to investigate the capabilities of the four-segment MWPC fabricated under tokamak plasma environments.

REFERENCES

[1] S. G. Lee, J. G. Bak, M. Bitter, K. Hill, U. W. Nam, Y. J. Kim and M. K. Moon, Rev. Sci. Intrum. **75**, 3693 (2004).
[2] S. G. Lee, J. G. Bak, M. Bitter, M. K. Moon, U. W. Nam, K. C. Jin, K. N. Kong and K. I. Seon, Rev. Sci. Instrum. **74**, 1997 (2003).
[3] A. M. Daltrini, M. Machida and M. J. R. Monteiro, Braz. J. Phys. **31**, 496 (2001).
[4] M. Bitter, S. von Goeler, R. Horton, M. Goldman, K. W. Hill, N. R. Sauthoff and W. Stodiek, Phys. Rev. Lett. **42**, 304 (1979).
[5] M. Bitter, K. W. Hill, B. Stratton, A. L. Roquemore, D. Mastrovito, S. G. Lee, J. G. Bak, M. K. Moon, U. W. Nam, G. Smith, J. E. Rice, P. Beiersdorfer and B. S. Fraenkel, Rev. Sci. Instrum. **75**, 3660 (2004).
[6] S. Han, H. Kang, Y. Kim, B. Moon, C. Chung, H. Cho and S. Kang, J. Korean Phys. Soc. **41**, 674 (2002).
[7] U. W. Nam, S. G. Lee, J. G. Bak, M. K. Moon, J. K. Cheon and C. H. Lee, Rev. Sci. Intrum. **78**, 103504 (2007).
[8] S. G. Lee, J. G. Bak, U. W. Nam, M. K. Moon and J. K. Cheon, Rev. Sci. Intrum. **78**, 063504 (2007).
[9] Glenn F. Knoll, *Radiation Detection and Measurement*, 3rd ed. (Wiley, Ann Arbor, 1999), p. 58.
[10] Glenn F. Knoll, *Radiation Detection and Measurement*, 3rd ed. (Wiley, Ann Arbor, 1999), p. 121.